Growth rate and frequency dispersion characteristics of drift waves in an r.f. collisional plasma

1972 J. Phys. A: Gen. Phys. 5 1095

(http://iopscience.iop.org/0022-3689/5/7/018)

J. Phys. A: Gen. Phys., Vol. 5, July 1972. Printed in Great Britain.

Growth rate and frequency dispersion characteristics of drift waves in an RF collisional plasma

B E KEEN and M W ALCOCK

UKAEA Research Group, Culham Laboratory, Abingdon, Berkshire, UK

MS received 22 November 1971

Abstract. Results are presented for a low frequency selfexcited oscillation in an inhomogeneous RF collisional plasma. In this plasma the radial electric field is very small, so that the resulting plasma rotation can be neglected, thus simplifying the interpretation of the experimentally measured frequencies. The oscillations occurred as azimuthally propagating waves with predominantly $m = +1$ mode number, and as standing waves in the axial direction with approximately half a wavelength in the tube. The frequency ω was dependent on the tube length, the axial magnetic field, and the gas neutral pressure, and measurements have been made in both helium and hydrogen plasmas while varying these parameters.

By using a method of dynamic stabilization to reduce the instability to a low level frequency measurements have been made in the linear regime where most linearized theories apply. Also, by analysing the subsequent return of the oscillations to its saturation level, the linear growth rate has been obtained. Comparison of these growth rate and frequency measurements in the linear regime with a previous theory of the drift-dissipative instability shows reasonably good agreement.

1. Introduction

In recent years, there has been considerable interest both theoretically and experimentally in the electrostatic branch of low frequency waves in an inhomogeneous magnetoplasma. An important group of these waves are the drift waves, whose presence depends upon a plasma density gradient perpendicular to a homogeneous containing magnetic field. Under certain plasma conditions, these waves can occur as propagating waves in a direction predominantly mutually perpendicular to the magnetic field and to the density gradient, in the selfoscillatory or 'instability' state. In this situation the waves have a positive growth rate, caused by collisions or lack of collisions between plasma particles, and thus grow in amplitude to a value which is only limited by nonlinear mechanisms in the plasma. The properties of these drift instabilities in both the collisional and collisionless regions have been summarized by Kadomtsev (1965) and Mikhailovski (1967). The importance of these waves is due mainly to the possible relationship between the presence of these instabilities and the anomalous cross-field plasma diffusion, which is enhanced above the loss value expected from classical binary-collision diffusion. In this respect, drift waves are predicted to occur at frequency values ω which are low with respect to the ion cyclotron frequency Ω_i ($\omega \ll \Omega_i$), and thus can convect ions across the magnetic field lines. Also, the growth rates γ are predicted to be large ($\gamma \simeq \omega$), and so the instability amplitude grows to relatively large proportions, and with this so does the net radial transport of particles associated with the fluctuating electric field of the

unstable waves. Consequently, both these factors pose a threat to plasma confinement and tend to increase the anomalous diffusion.

Attempts to compare measured drift instability characteristics with theory have been complicated by two main experimental factors. These are:

(i) In most reported experimental observations of drift waves large radial electric fields E_r have existed in a plasma column as well as a radial density gradient. This radial electric field E_r taken together with an axial magnetic field, leads to an azimuthal drift of plasma. This drift causes the plasma column to rotate, and, consequently, leads to a Doppler shift in the predicted instability frequency, usually of the same order of magnitude as the instability frequency itself (Hendel *et al* 1968, Enriques *et al* 1968 and Rowberg and Wong 1970). Also, it has been shown (Aldridge and Keen 1970) that a rotationally convected drift instability can be sustained in the presence of a radial electric field in the collisional regime. However, some experiments have been performed (Alcock and Keen 1971a) in an afterglow of plasma in which this electric field is very small and can be neglected.

(ii) Most theories with which the experimental results are compared are linearized theories, whereas most experiments have been performed on selfsustained oscillations which are amplitude limited by nonlinear mechanisms. Thus the experimental results are obtained in the nonlinear, large amplitude regimes, and it is not obvious that a direct comparison can be made with a linear theory. Some experimental results (Rowberg and Wong 1970) have been obtained in the linear, small amplitude regime, but in this case a radial electric field existed, too.

This paper reports experiments which were performed on a low frequency self-oscillatory instability in an RF discharge, in which the radial electric field was extremely small ($\simeq 0 \pm 0{\cdot}01$ V cm^{-1}). The RF discharge was obtained in a field free region and so the major causes of instability such as unidirectional current flow, and imposed electric fields were absent. Experiments were performed using a dynamic stabilization technique (Alcock and Keen 1971b) to suppress the instability or reduce it to a small amplitude. In this way, the instability characteristics were measured in the linear regime, and allowed the linear growth rate (γ) of the instability to be measured as its amplitude was allowed to return to its nonlinear saturation value. Experiments were performed in both helium and hydrogen plasmas, at various magnetic field values, and as a function of the background neutral pressure in each case. The instability frequency ω was measured as the axial wavelength ($\lambda_z = 2\pi/k_z$) was varied, and this allowed the ($\omega - k_z$) dispersion relationship to be constructed.

Section 2 develops the theory of the drift-dissipative instability (Timofeev 1963a, 1963b and Alcock and Keen 1971a) in which both electron–neutral and ion–neutral collisions are included. Section 3 describes the apparatus and the diagnostic methods employed to determine the DC plasma properties and the characteristics of the instability. The results obtained on the instability as a function of column length, axial magnetic field and neutral pressure are reported in § 4. Finally, § 5 compares these results with the foregoing theoretical predictions, and briefly discusses the conclusions reached.

2. Theory

The stability of an inhomogeneous plasma column in a uniform axial magnetic field, in which both electron–neutral and ion–neutral collisions are included, has been considered by Timofeev (1963a and 1963b) and further extended by Alcock and Keen (1971a).

The plasma behaviour was described by using the equations of motion of the ions and electrons including collisions, taken together with the equations of continuity of each species. These equations were considered in the following approximations:

(*a*) The 'slab' model was adopted in the 'localized' approximation.

(*b*) These equations were linearized to first order such that small oscillatory perturbations of density n^1 and potential ϕ^1, propagated. The perturbations were of the form $\exp-(\omega t-\boldsymbol{k}\,.\,\boldsymbol{r})$, where ω is the oscillation frequency and $\boldsymbol{k}$ is the wavevector.

(*c*) The calculation was developed in the case of oblique propagation to the magnetic field $\boldsymbol{H}$, in which it was assumed that $k_y \gg k_x$, k_z, $(1/n_0)(\mathrm{d}n_0/\mathrm{d}x) = \kappa$ (the inverse scale length). Here, $\boldsymbol{H}$ was taken to be uniform in the z direction, while the density gradient was assumed to be along the 'x' direction.

(*d*) The low frequency approximation was considered in which the oscillation frequency, $\omega \ll \Omega_i$ ($\Omega_i = eH/Mc$ is the ion cyclotron frequency).

(*e*) The equations of motion were formulated in the nonisothermal case in which $T_e \gg T_i$ (T_e and T_i are the electron and ion temperatures respectively, measured in energy units (eV)), and the ion temperature T_i is taken to be very small. Implicit in representing the electron motions by a single temperature T_e is the assumption that these motions have a maxwellian distribution of velocities. Consequently, no instabilities due to a nonmaxwellian distribution can be predicted by this theory.

(*f*) It was assumed that there were no zero order electric fields E_0 present in the plasma (ie $E_0 = -\nabla\phi_0 = 0$, where ϕ is the electric potential), and further that the magnetic field and neutral pressures values were such that the ion–neutral and electron–neutral collision frequencies, ν_i and ν_e respectively, satisfied the inequalities, $\nu_i \ll \Omega_i$, and $\nu_e \ll \Omega_e$.

In the electron equation of motion, the electrons were taken to be inertialess, and then this equation reduces to

$$T_e\frac{\nabla n_e}{n_e} - e\nabla\phi + \frac{e}{c}(\boldsymbol{v}_e \times \boldsymbol{H}) + m\boldsymbol{v}_e\nu_e = 0 \tag{1}$$

where n_e is the electron density, and $\boldsymbol{v}_e$ the electron velocity. By using the electron equation of continuity

$$\frac{\partial n}{\partial t} + \nabla\,.\,(n_e\boldsymbol{v}_e) = 0 \tag{2}$$

the electron velocity can be eliminated between equations (1) and (2). If only terms linear in $\beta = \nu_e/\Omega_e$ are retained in the linearized equations, a relationship between n^1 and ϕ^1 is obtained given by

$$\left(\frac{n_e^1}{n_{e0}}\right) = \frac{k_z^2 - \mathrm{i}\beta k_y\kappa(1-\beta k_x/k_y)}{k_z^2 D_e - \mathrm{i}\omega}\,\frac{e\phi^1}{m\nu_e} \tag{3}$$

where $D_e = T_e/m\nu_e$ is the electron diffusion coefficient.

Similarly, the ion equation of motion, in which ion inertia is included and ion temperature is ignored is given by

$$M_i\frac{\mathrm{d}\boldsymbol{v}_i}{\mathrm{d}t} = -e\nabla\phi + \frac{e}{c}(\boldsymbol{v}_i \times \boldsymbol{H}) - M_i\boldsymbol{v}_i\nu_i\,. \tag{4}$$

The ion equation of continuity

$$\frac{\partial n_i}{\partial t} + \nabla \cdot (n_i \boldsymbol{v}_i) = 0 \tag{5}$$

is used to eliminate the ion velocities $\boldsymbol{v}_i$, between the linearized equations (4) and (5). The following expression relating n_i^1 and ϕ_1 results, giving:

$$\left(\frac{n_i^1}{n_{i0}}\right) = \left(\frac{(ik_x\kappa - k_\perp^2)(\omega + iv_i)}{\Omega_i} - k_y\kappa\right)\frac{e\phi^1}{M_i\Omega_i\omega} \tag{6}$$

where

$$k_\perp^2 = (k_x^2 + k_y^2).$$

The electron and ion density perturbation n_e^1 and n_i^1 can be eliminated by using Poisson's equation, $\nabla^2\phi = 4\pi e(n_i - n_e)$. In this case, if the principle of quasineutrality ($n_{i0} = n_{e0}$) is assumed, to the order of approximation in this theory, $n_e^1 = n_i^1$. Then, by eliminating n^1 and ϕ^1, from equations (3) and (6), the dispersion relationship relating ω and k can be obtained, which reduces to

$$\omega^2 + \omega\left\{\frac{x\omega_s}{1+x^2} + i\left(k_z^2 D_e + \nu_i + \frac{\omega_s}{1+x^2}\right)\right\} - k_z^2 D_e \nu_i + \frac{x\omega^*\omega_s}{1+x^2} + i\frac{\omega_s\omega^*}{1+x^2} = 0 \tag{7}$$

where

$$\omega^* = \frac{k_y c T_e \kappa}{eH} \qquad x = \frac{\kappa k_x}{k_\perp^2} \qquad \omega_s = \frac{k_z^2 \Omega_e \Omega_i}{k_\perp^2 \nu_e}.$$

This quadratic dispersion equation can be solved and expressions relating the propagation frequency $\mathrm{Re}(\omega)$ and the growth rate $\gamma = \mathrm{Im}(\omega)$, to the physical parameters such as magnetic field, wavenumbers, and electron and ion collision frequencies. When the values of these physical parameters are substituted into the equation, values can be computed for $\mathrm{Re}(\omega)$ and the growth rate (γ), as a function of axial wavenumber k_z, magnetic field H, and neutral pressure p. Some of these theoretically predicted variations are shown in figures 3–6.

In general, theory indicates that for the variation of the propagation frequency $\mathrm{Re}(\omega)$ as a function of axial wavenumber k_z that at high wavenumbers, the frequency tends to the drift frequency ω^* whereas at low k_z, the frequency tends to zero value. Values for the growth rate γ indicate that the important collisions for instability are the electron–neutral collisions, whereas the stabilizing influence comes from ion–neutral collisions. In this way, there appears to be only a certain range of axial wavenumbers (or wavelengths) for which positive growth and thus instability is apparent (see figure 3).

3. Experimental details

The experiment was performed in a continuously running RF plasma, which was produced in the apparatus shown schematically in figure 1. An RF discharge was formed between a plate and an earthed grid at one end of the discharge tube ($\simeq 5$ cm diameter). The plasma diffused through this grid into a longitudinal electric field-free region between

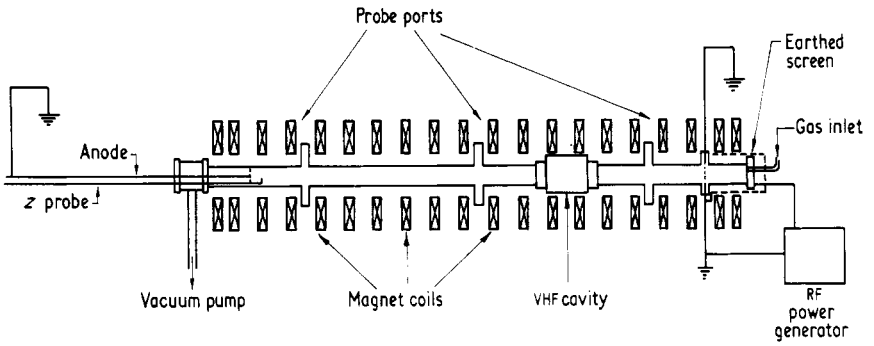

Figure 1. Schematic diagram of RF discharge apparatus.

this grid and a movable earthed 'anode' plate, which allowed the plasma length to be varied (maximum length $\simeq 180$ cm). The longitudinal magnetic field in the plasma volume was uniform ($\simeq 0{\cdot}5\%$) and could be varied over the range 0·1–3·2 kG. The discharge was run in either He or H_2 gas which was introduced into the tube through a needle valve at the production end of the apparatus, and flowed through the tube continuously during an experiment. The neutral pressure in the discharge tube was maintained at a constant value by fine adjustment of the gas flow rate and by varying the pumping rate at the opposite end of the apparatus. The neutral pressure was measured on a Pirani gauge which had been previously calibrated against a McLeod gauge for the particular gas used.

Spaced along the glass discharge tube were various ports, as indicated in figure 1. These ports were spaced apart azimuthally by 90°, and allowed various interchangeable probes which could be moved radially, to be inserted at these points along the plasma. A longitudinal probe was inserted from the 'anode' end, and this moved such that it traversed the whole length of the column.

A UHF cavity, coaxial with the glass tube, was used for measuring the average electron density and also, for obtaining the electron–neutral collision frequency. This cavity which was 15 cm diameter and 10 cm long was operated in its TM_{010} mode and had a resonant frequency of 1320 MHz. In order to determine the electron density, its resonant frequency (f_0) was measured without plasma present. Then the plasma discharge was set running through the cavity and the change in resonant frequency Δf noted. This change, Δf, has been related to the electron density n by Agdur and Enander (1962) using a perturbation analysis giving

$$\frac{\Delta f}{f_0} = F_r\left(\frac{r_1}{r_2}\right)^2\left(\frac{f_p}{f_0}\right)^2 \tag{8}$$

where F_r is a form factor dependent on the geometry of the cavity and plasma, r_1 and r_2 are the radii of plasma and cavity respectively, and $f_p = (4\pi ne^2/m)^{1/2}$ is the plasma frequency. However, the form factor F_r cannot be predicted with great accuracy when large holes are present in the end of the cavity, and when a thick glass walled tube is used. In this situation calibration with a known dielectric constant is desirable (Keen and Fletcher 1971). In this case, the cavity was calibrated using expanded polystyrene (dielectric constant $\epsilon \simeq 1{\cdot}015$).

The collision frequency for electrons ν_e can be estimated by measuring the change in the quality factor Q of the cavity. Buchsbaum and Brown (1957) have shown that the following relationship is obtained:

$$\frac{1}{Q}-\frac{1}{Q_0}=\frac{\nu_e \Delta f}{\pi f_0^2} \tag{9}$$

where Q_0 is the unloaded value of the cavity and Q is that value with plasma present.

When this coaxial cavity was removed from the glass tube, four equally spaced conductors parallel to tube axis were strapped to the outside of the tube. By passing an 'in-phase' oscillating current ($\simeq 1$ MHz) through these conductors, an oscillating azimuthal magnetic field H_ϕ could be induced in the plasma. For values of $H_\phi/H_0 \simeq 1\%$, stabilization or partial suppression of any instability was observed (Alcock and Keen 1971b). This technique allowed the instability frequency to be measured at low amplitude and thus in the linear regime. Subsequently, growth of the instability occurred when the field H_ϕ was removed, and so the instability growth rate could be measured.

4. Results

4.1. DC measurements

A radially moving double Langmuir probe was used to measure the density and electron temperature (T_e) profiles (Johnson and Malter 1950). The peak density n_0 was found to vary depending upon the power output from the RF generator and the neutral gas used (He or H_2), but typical values in the range $1\text{–}5 \times 10^9$ cm^{-3} were obtained. A typical density profile is shown in figure 2(*a*) which was taken in a helium plasma. Over a radial range 0·4–2·0 cm the inverse density scale length $\kappa = (1/n)(\partial n/\partial r)$ was constant and typical values of $\kappa = 0{\cdot}70$ cm^{-1} for He and $\kappa = 0{\cdot}40$ cm^{-1} for H_2 plasmas were obtained. The electron temperature T_e measured on the same probe again varied as a function of RF power and neutral gas, in the range 3–8 eV and typical values of 6·5 eV in He and 3·5 eV in H_2 were obtained. The electron temperature was found to be constant in the radial range 0–2·0 cm, but outside this range the temperature fell rapidly near the wall. The electron temperature was checked using a single probe, and consistent values were obtained by these two methods. Good straight line plots of $\ln i_e$ against voltage (V_a) applied to the probe, were obtained, below saturation current, where i_e is the electron current. This tends to suggest that the electron velocity distribution is close to maxwellian, as assumed in the theory. A further check was made on the electron temperature with the stabilizing field H_ϕ present ($H_\phi/H_0 \simeq 1\%$), and with it removed. No effect was observed within the accuracy of the measurement ($\simeq \pm 0{\cdot}2$ eV).

The floating potential ϕ_f of the plasma was measured on a high impedance digital voltmeter as a function of radius and was found to vary less than 1 mV across the column radius, as shown in figure 2(*b*). However, the radial electric field E_r is related to the floating potential by the relationship

$$E_r = -\frac{\partial \phi_p}{\partial r} = -\frac{\partial}{\partial r}(\phi_f+\phi_s) = -\frac{\partial}{\partial r}\left\{\phi_f+\frac{T_e}{2}\ln\left(\frac{\pi \nu_e}{\Omega_e}\frac{M}{m}\right)\right\}$$

$$= -\frac{\partial}{\partial r}(\phi_f + A T_e) \tag{10}$$

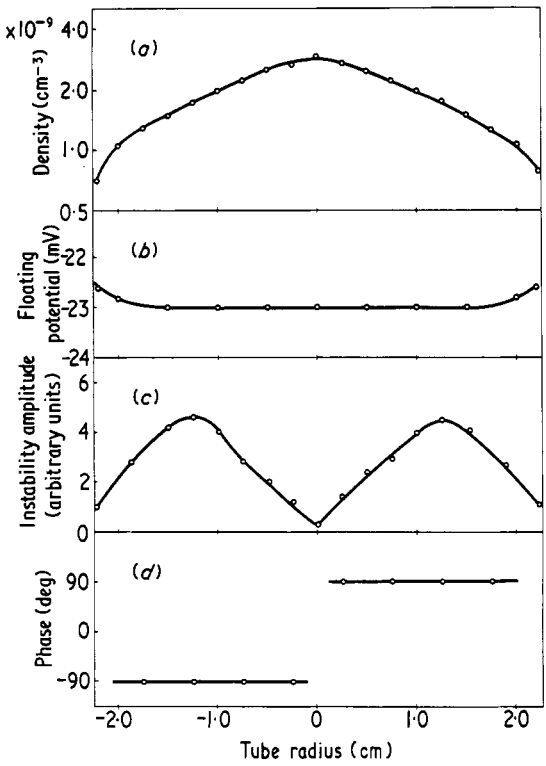

Figure 2. (*a*) Density, (*b*) floating potential, (*c*) instability amplitude and (*d*) phase angle, as functions of tube radius taken in a helium plasma.

where ϕ_p is the plasma potential, ϕ_s the sheath potential, and A is a constant (Aldridge and Keen 1970). Since both ϕ_f and T_e were independent of radius, the radial electric field was found to be $E_r = 0 \pm 0{\cdot}01$ V cm^{-1}. Theoretically, Timofeev (1963a) has shown that in a plasma of this type, an ambipolar radial electric field is set up such that the net electric current to a dielectric wall is zero and then the radial electric field value is given by

$$E_r = -\kappa T_e \left\{ 1 + \left(\frac{\Omega_e \Omega_i}{\nu_e \nu_i} \right) \right\}^{-1}. \tag{11}$$

Under the conditions used in these experiments, typical theoretical values of $E_r \simeq 2\text{–}5 \times 10^{-4}$ V cm^{-1} result, which is not in contradiction with the measured values. Consequently, any plasma rotation due to this field should be small, and thus can be ignored.

The electron–neutral collision frequency was obtained by measuring the change in the 'Q' factor of the resonant UHF cavity coaxial with the discharge in the tube, and using equation (9) to determine its value. The change in $1/Q$ was checked as a function of neutral pressure p with both H_2 and He gases. A linear relationship was found between $1/Q$ and p, thus indicating that the effect was due to electron–neutral collisions. The final values obtained were (*a*) $\nu_e/p = 0{\cdot}70 \pm 0{\cdot}15 \times 10^9$ s^{-1} Torr^{-1} for H_2, and (*b*) $\nu_e/p = 0{\cdot}80 \pm 0{\cdot}15 \times 10^9$ s^{-1} Torr^{-1} for the He plasma.

On simple hard sphere kinetic theory considerations (Alcock and Keen 1971a) values of the ion–neutral collision frequency were computed and gave (*a*) $\nu_i/p = 2{\cdot}5 \pm 0{\cdot}15 \times 10^{-7}$ s^{-1} Torr^{-1} for H_2 and (*b*) $\nu_i/p = 2{\cdot}0 \pm 0{\cdot}15 \times 10^{7}$ s^{-1} Torr^{-1} for He. These values agree favourably with values calculated from ion mobility measurements (Brown 1959).

4.2. AC measurements

The properties of the instability were observed from the various floating and ion-biased probes distributed around and along the plasma column. The azimuthal properties of the wave were inferred from four probes spaced 90° apart around the tube. Figure 2(*b*) shows the variation of amplitude and figure 2(*c*) indicates the phase variation as a function of radius of the tube, taken across one diameter of the plasma. The results were consistent with a predominantly $m = +1$ propagating wave in the azimuthal direction.

The longitudinally moving probe was used to measure the axial phase and amplitude variation. These results indicated that the instability was a standing wave in the axial direction, with a half-wavelength ($\lambda/2$), in the tube length. This point seems to be similar to that observed in previous drift wave experiments (Hendel *et al* 1968 and Rowberg and Wong 1970) but in contrast to the experiments in an afterglow plasma (Alcock and Keen 1971a, 1971b) in which a standing wave of one whole wavelength in the tube was observed.

4.3. The dispersion relationship

When the external conditions (H, p, etc) had been arranged so that a selfoscillatory wave was present in the tube, the output from any of the probes was displayed on a spectrum analyser. This allowed the frequency and amplitude of the instability to be observed simultaneously. Then the magnetic field H and neutral pressure p were kept constant and the plasma length 'l' was changed thus varying the wavelength λ of the oscillation ($\lambda = 2l$) and consequently, the frequency ω. This allowed the relationship between the axial wavenumber, $k_z = 2\pi/\lambda$, and the frequency ω to be checked. Typical results are shown in figure 3(*a*) for helium, and in figure 3(*b*) for hydrogen. In these figures, the smallest value of k_z was determined by the maximum length of the tube, and the largest k_z value was determined by the smallest length of tube at which clear $m = +1$ modes were present. As the length of tube was reduced other modes appeared ($m \gtrsim 2$) and the spectrum became much more turbulent.

By using the dynamic stabilization method to reduce the amplitude of the density oscillation such that $n^1/n_0 \lesssim 5\%$ a check was made to observe the effect on the frequency, of large amplitudes in the plasma. The effect was found to be small, and in all cases the instability frequency increased as the amplitude decreased by $\lesssim 5\%$. Consequently, very little error is involved by taking frequency values under the nonlinear saturation amplitude conditions rather than those frequency values corresponding to the small amplitude, linear region.

Further measurements were made at a fixed plasma column length, and at constant neutral pressure, while the magnetic field was varied. Typical results are shown in figure 4(*a*) for helium and figure 4(*b*) for hydrogen. The lowest value of magnetic field used in these experiments was determined by that value at which the instability was still present in the plasma, and the highest field was determined by the value at which the instability was still a pure $m = +1$ mode only. For higher field values, multimode effects became apparent and made further measurements impossible.

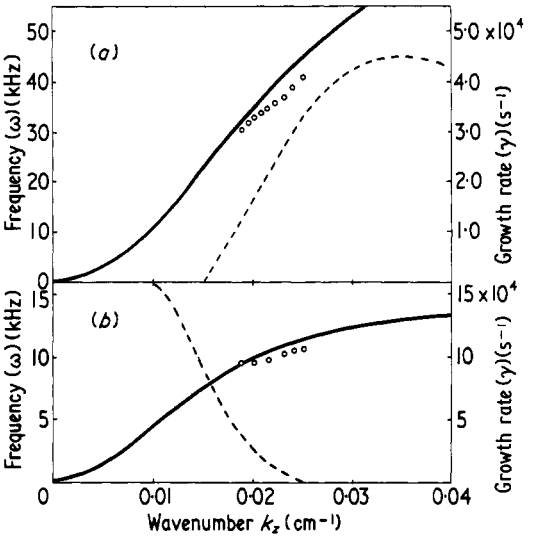

Figure 3. Dispersion diagram for (*a*) a helium plasma and (*b*) a hydrogen plasma taken at $H \simeq 200$ G. The full curve is the theoretical curve for ω against k_z and refers to the scale on the left hand side. The broken curve is the theoretical curve of the growth rate (γ) against k_z and refers to the right hand scale.

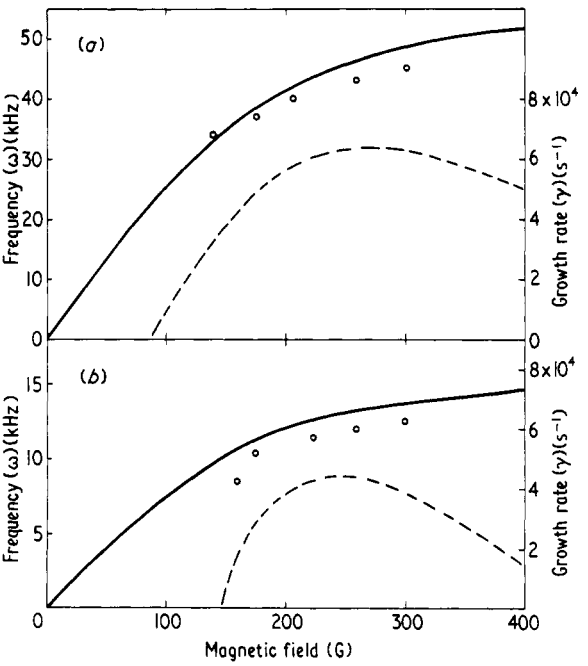

Figure 4. Instability frequency as a function of magnetic field at fixed tube length and constant neutral pressure for (*a*) a helium plasma and (*b*) a hydrogen plasma.

Finally, frequency measurements were made at constant magnetic field, and fixed tube length, while varying the neutral pressure in the tube. This had the effect of increasing both the electron–neutral (ν_e) and ion–neutral (ν_i) collison frequency linearly proportional to the neutral pressure (p). Results are shown in figure 5(a) for helium and figure 6(a) for hydrogen. Again, the highest pressure used was determined by the value at which growth of the instability still occurred (ie $\simeq 13$ mTorr for He, and $\simeq 10$ mTorr for H_2), while the lowest value was determined by that value at which other modes began to dominate and a multimode spectrum took over.

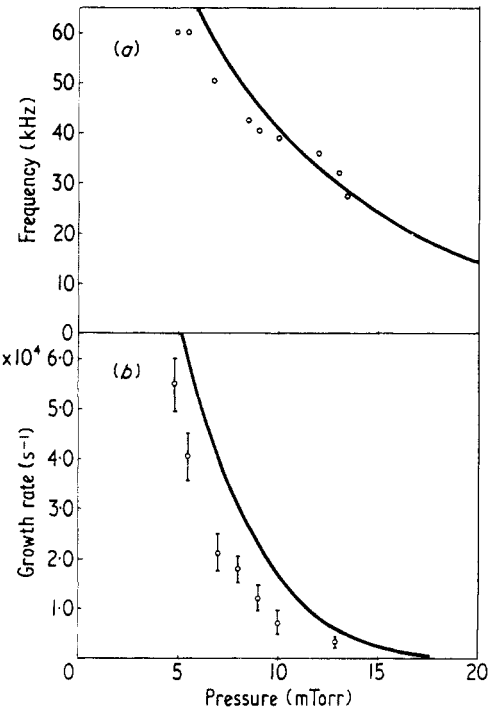

Figure 5. (a) Instability frequency and (b) instability growth rate as a function of neutral pressure in a helium plasma. The full curves are from theory.

4.4. Growth rate measurements

By gating the RF current applied to the suppressor conductors on the outside of the tube, the stabilizing field H_ϕ could be switched on and off at periodic intervals. This caused the instability to be suppressed and then subsequently grow to its amplitude saturation value, periodically. A typical trace obtained in this way is shown in figure 7 (plate). Analysis of traces enabled the linear growth rate (γ), to be obtained under various conditions in the plasmas. Plots of relative amplitude ($a/a_0(p)$) as a function of time obtained for the growing part of the signal are shown in figure 8, taken in the helium plasma at different neutral pressure values of $p = 10$ mTorr (curve A), $p = 9$ mTorr (curve B), and $p = 7$ mTorr (curve C). The growth rates measured as a function of neutral pressure, are shown in figure 5(b) for a helium plasma, and in figure 6(b) for a hydrogen plasma.

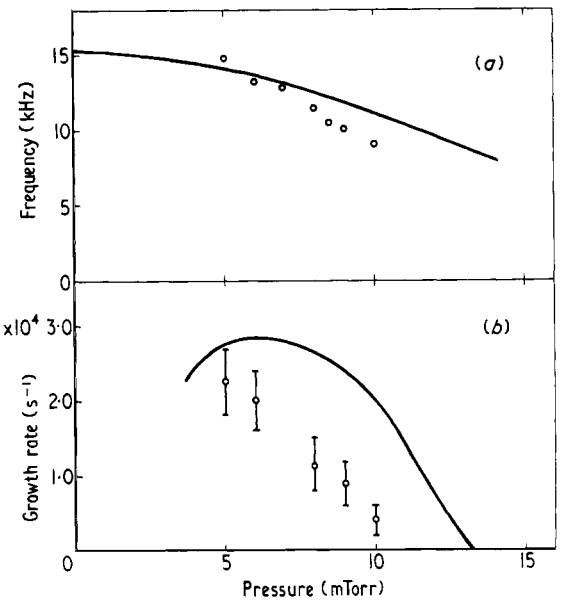

Figure 6. (*a*) Instability frequency and (*b*) instability growth rate as a function of neutral pressure in a hydrogen plasma. The full curves are from theory.

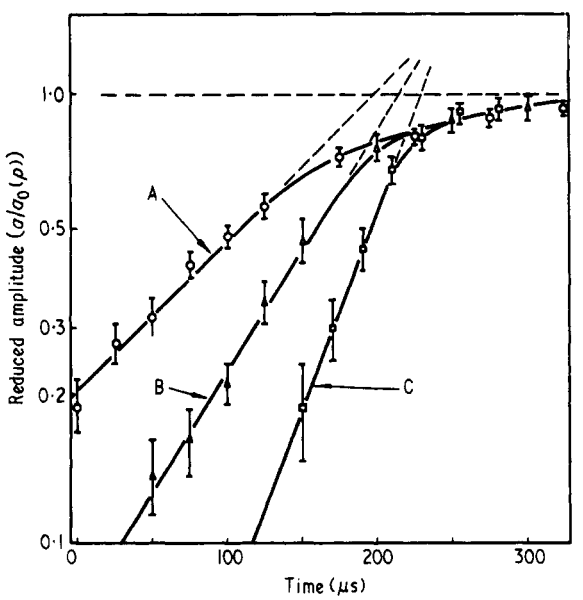

Figure 8. Reduced instability amplitude ($a/a_0(p)$) as a function of time for three neutral pressures: A p = 10 mTorr, B p = 9 mTorr and C p = 7 mTorr in the helium plasma.

5. Discussion and conclusions

The theoretical variation of the frequency Re(ω) and the linear growth rate γ = Im(ω) for the drift-dissipative instability as a function of the externally variable parameters,

tube length ($\propto k_z$), magnetic field, and neutral pressure has been computed from the dispersion relationship in equation (7). The full curves in figure 3(*a* and *b*) show the theoretical curves ω against k_z calculated from this equation for (*a*) a helium plasma and (*b*) a hydrogen plasma using the particular parameter values appropriate to each case. The open circles in the figures are the experimental points which are restricted to certain k_z values for the reasons explained in § 4.3. It is seen that reasonable agreement is achieved in this situation.

The broken lines in these figures indicate the theoretical growth rate values (γ against k_z) calculated from the dispersion equation (equation (7)), and these curves refer to the right hand scale. Positive values of growth rate γ indicate the region in which the instability should be present, and it is seen that where measurements have been possible, they occur in this positive growth rate region.

Similarly, in figure 4, results are shown for the frequency values ω measured as a function of the applied magnetic field H (*a*) for a helium, and (*b*) for a hydrogen plasma. Again, the full curve is the theoretical ω against H plot and the broken curve is a plot of the growth rate against field. In this case, good agreement is apparent and the instability is observed in the region where a positive growth rate is predicted.

In figure 5(*a*) the experimental points are plotted as open circles, whereas the full curve is the theoretical curve for the frequency ω against the neutral pressure in the tube, in the case of a helium plasma. Similarly, in figure 6(*a*), the results are shown for a hydrogen plasma. Again relatively good agreement is achieved.

Figure 5(*b*) indicates the experimental values of the growth rate γ as a function of neutral pressure in the helium plasma. The full curve, again, shows the theoretically computed values. Similarly, figure 6(*b*) shows the corresponding results for the hydrogen plasma. In these cases, the agreement between experiment and theory is not so good for the growth values.

However, in comparing experiment and theory, certain limitations of the theory must be borne in mind. These are:

(*a*) The stability calculation has been made in 'slab' or cartesian geometry, and the cylindrical case has been approximated by assuming that $x \to r$, $y \to r\theta$, and $z \to z$. Therefore k_y is taken as m/r_0, where 'm' is the azimuthal mode number, and r_0 corresponds to the radius at which the instability has maximum amplitude. In order for this approximation to be satisfied, k_y should be large compared with the inverse scale length κ, that is, $r_0\kappa/m \ll 1$. In these experiments, $r_0\kappa/m \simeq 0{\cdot}7$ is the worst case, and this is a point of divergence between experiment and theory.

(*b*) The theoretical model is based upon the 'localized' approximation, which is only satisfied, again, if $r_0\kappa \ll 1$. As mentioned previously, this is not entirely satisfied experimentally.

(*c*) Other approximations involved are $\nu_e/\Omega_e \ll 1$, $\nu_i/\Omega_i \ll 1$, and $\omega/\Omega_i \ll 1$. The condition $\nu_e/\Omega_e \ll 1$ is well satisfied in all cases, whereas the worst situations occur in helium for the other conditions, which are $\nu_i/\Omega_i \simeq 0{\cdot}3$ and $\omega/\Omega_i \simeq 0{\cdot}5$. Again, these represent some limitations in comparing theory and equipment.

(*d*) In the calculation, the value of the growth rate γ depends upon taking the difference between large terms which are of the same order of magnitude, thus leaving a remainder which is a smaller quantity. However, the real part of the frequency ω involves the sum of large terms and thus the growth rate is subject to a larger error than the frequency values.

In conclusion, experiments have been conducted in a region where the usual causes of instability such as longitudinal current or electric field, radial electric field, magnetic

field gradient, temperature gradient, etc are absent. In fact, the predominant excitation mechanism for instability remaining is the azimuthal electron drift created by the radial density gradient and the longitudinal magnetic field. The experiments have been performed in the linear regime, by partially suppressing the instability by a method of dynamic stabilization, and further, direct measurements have been made of the linear growth rates. The dispersion relationship of the waves has been obtained in two different plasmas (He and H_2) as a function of external magnetic field, axial wavenumber, and neutral gas pressure. The results obtained have been compared with the theory of the drift-dissipative instability (Timofeev 1963a and 1963b). Comparison between this theory and the experimental results shows reasonably good agreement, in view of the limitations inherent in the theory, and the probable error in the experimental results. Therefore it is concluded that the observed instability is the drift-dissipative instability.

References

Agdur B and Enander B 1962 *J. appl. Phys.* **33** 575–81
Alcock M W and Keen B E 1971a *Phys. Rev.* A **3** 1087–96
—— 1971b *Phys. Rev. Lett.* **26** 1426–9
Aldridge R V and Keen B E 1970 *Plasma Phys.* **12** 1–16
Brown S C 1959 *Basic Data of Plasma Physics* (New York: Wiley)
Buchsbaum S J and Brown S C 1957 *Phys. Rev.* **106** 196–201
Enriques L, Levine A M and Righetti G B 1968 *Plasma Phys.* **10** 641–4
Hendel H W, Chu T K and Politzer 1968 *Phys. Fluids* **211** 2426–39
Johnson E O and Malter L 1950 *Phys. Rev.* **80** 58–68
Kadomtsev B B 1965 *Plasma Turbulence* (New York: Academic Press)
Keen B E and Fletcher W H W 1971 *J. Phys.* D: *Appl. Phys.* **4** 1695–702
Mikhailovski A B 1967 *Rev. Plasma Phys.* **3** 159–227
Rowberg R E and Wong A Y 1970 *Phys. Fluids* **13** 661–71
Timofeev A V T 1963a *Zh. tekher. Fiz.* **33** 909–14 (1964 *Sov. Phys.–Tech. Phys.* **8** 862–5)
—— 1963b *Dokl. Akad. Nauk.* **152** 84–7 (1964 *Sov. Phys.–Dokl.* **8** 890–2)

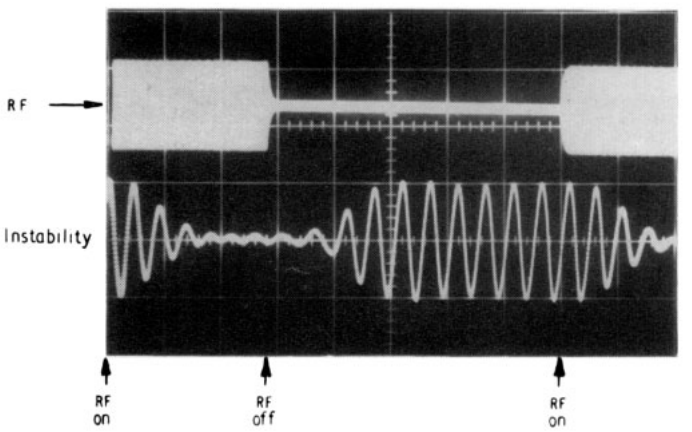

Figure 7. Upper trace shows sequence of applied RF currents to stabilizing system, and lower trace shows its effect on the instability amplitude.